

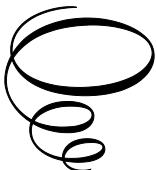
Derivative Spectroscopy

Derivative Spectroscopy

By

Joseph Dubrovkin

Cambridge
Scholars
Publishing



Derivative Spectroscopy

By Joseph Dubrovkin

This book first published 2021

Cambridge Scholars Publishing

Lady Stephenson Library, Newcastle upon Tyne, NE6 2PA, UK

British Library Cataloguing in Publication Data

A catalogue record for this book is available from the British Library

Copyright © 2021 by Joseph Dubrovkin

All rights for this book reserved. No part of this book may be reproduced, stored in a retrieval system, or transmitted, in any form or by any means, electronic, mechanical, photocopying, recording or otherwise, without the prior permission of the copyright owner.

ISBN (10): 1-5275-6348-0

ISBN (13): 978-1-5275-6348-3

TABLE OF CONTENTS

Preface.....	ix
--------------	----

About the Structure of the Book	xi
---------------------------------------	----

Abbreviations.....	xiii
--------------------	------

PART I: MATHEMATICAL DERIVATIVES OF ANALYTICAL SIGNALS

Introduction	2
--------------------	---

Chapter One.....	3
------------------	---

Symmetrical Peak Shapes in Spectroscopy and Chromatography	
--	--

Chapter Two	7
-------------------	---

Mathematical Derivatives of Typical Peaks	
---	--

Chapter Three	30
---------------------	----

Analysis of Noise in Spectral Measurements	
--	--

Chapter Four	36
--------------------	----

Resolution Limit in Derivative Spectroscopy	
---	--

Chapter Five	53
--------------------	----

Information Content of the Derivative Spectrum	
--	--

PART II: DERIVATIVE SPECTROSCOPY TECHNIQUES

Introduction	60
--------------------	----

Chapter One.....	61
------------------	----

Analog Differentiation	
------------------------	--

Chapter Two	66
-------------------	----

Digital Differentiation: Finite Differences	
---	--

Chapter Three	72
Digital Differentiation: Savitzky-Golay filters	
Chapter Four	96
Smoothing and Differentiation Using the Fast Fourier Transform	
Chapter Five	111
A Hypothetically Optimal Non-Recursive Smoothing Filter	
Chapter Six	119
Smoothing and Differentiation Using a Regularized Continuous Fourier Transform	
Chapter Seven	133
Smoothing with Splines	
Chapter Eight.....	139
Differentiation Using Wavelets	
Chapter Nine.....	151
Optical Differentiation: Slit Monochromators	
Chapter Ten	167
Laser Modulation Spectroscopy	
PART III: ANALYSIS OF POORLY-RESOLVED SPECTRA STRUCTURE USING MATHEMATICAL DIFFERENTIATION	
Chapter One.....	175
Peak Detection	
Chapter Two	182
Errors of the Peak Maximum Identification in the 2 nd -Order Derivative	
Chapter Three	196
Determination of the Peak Intensities and Width in the 2 nd -Order Derivative	
Chapter Four.....	216
Determination of Doublet Parameters Using the Empirical Coefficients of the 2 nd -Order Derivative	

PART IV: QUANTITATIVE DERIVATIVE SPECTROMETRY

Introduction	228
Chapter One.....	229
Intensity Measurements: Relationships between Analyte Concentration and Intensity	
Chapter Two	244
Applications of Quantitative Derivative Spectrometry in the Industrial Laboratory	
Chapter Three	251
The Selectivity of Quantitative Derivative Spectrometry	
Chapter Four.....	257
Informational Aspects of the Quantitative Derivative Spectrometry	

**PART V: DIFFERENTIATION OF THE ANALYTICAL SIGNALS:
INDUSTRIAL AND SCIENTIFIC APPLICATIONS**

Introduction	264
Chapter One.....	265
The Derivative Technique in Different Types of Spectroscopy: Technical Features and Advantages	
Chapter Two	288
Derivative Recording of Analytical Signals Excluding Optical Spectroscopy	
Appendix A	297
Analytical Signal Processing using Fourier Transform and Splines	
Appendix B.....	305
Differentiation of the PMG and Dobosz Functions	
Appendix C.....	307
Noise	

Appendix D	309
Estimation of the Information Measure of the Resolution	
Appendix E.....	312
RC Circuits	
Appendix F.....	314
Combination of the Triangle Multi-Pass Moving Average Filter with the 2 nd -Order Differentiation	
Appendix G	316
Tikhonov Regularization	
Appendix H	318
Estimation of the Optimal Filter for a Linear Signal	
Appendix I.....	320
Tables to Chapter 2.6	
Appendix J.....	327
Lock-In Amplifier	
Appendix K	328
Laser Diodes	
Appendix L.....	332
Signal Shapes and their Derivatives in Electrochemical Analysis	
Appendix M.....	335
Spectroscopy	
Appendix SW	345
MATLAB Programs	
Bibliography	381
Index	439

PREFACE

The second half of the 20th century witnessed impressive technological advances triggered by the arms and space races between the Soviet Union and the United States. This rivalry stimulated significant progress in physical and chemical sciences, which required the improvement of traditional analytical methods and the creation of high-speed, highly effective instrumental techniques. Analog electronic devices were replaced by digital computerized tools managing large quantities of information, which, in turn, gave impetus to the emergence of a new discipline - chemometrics.

Chemometrics uses statistical and mathematical methods for processing data obtained by analytical instruments to extract maximum useful information. The first stage of this process, named preprocessing, usually includes data denoising, decomposition of complex numerical objects (vectors and matrices) into independent components, and background elimination.

One of the first chemometrics applications was the differentiation of analytical signals in electrochemical analysis, spectroscopy, and chromatography. In parallel, physicists developed the theory and technology of modulation spectroscopy, which has numerous mutual features with the derivative method. Spectroscopy stimulated the implementation of the modulation technique in analytical instrumentation.

Derivative Spectroscopy (DS) originated in the 1950s with the development of the electronic differentiators and optical modulation devices. Later, digital differentiation has become a priority. The most attractive features of the DS are:

1. Artificial improvement of the resolution of the analytical instruments.
2. Appearance of peaks and zero points suitable for analysis in the presence of interferences
3. Suppression of background.

The main advantage of the modulation technique is a significant improvement of the analytical sensitivity due to the remarkable noise reduction.

Numerous researches in the field of the DS were summarized in our short monograph, published in 1988 in Russian [1]. This study included theory, techniques, and analytical applications of the derivative methods. It

was intended for a broad audience of students and professionals in physics, chemistry, and signal processing. After a few years, G. Talsky published a new book that provided analysts with useful introductions to the subject [2]. For the last three decades, the DS has continued to develop, mainly, in the field of the digital differentiation and its combination with other processing procedures.

The derivative technique was briefly reviewed by the leaders in chemometrics [3-6].

Summing up the results of more than half a century of research in the field of DS, we decided to prepare a new monograph that includes all fundamental problems of this method.

The present study is an attempt to give a detailed explanation of the reached theoretical and numerical results. The goal (similar to our previous book [7]), was to avoid the blind faith of readers in the reliability of the conclusions and recommendations.

Theoretical discussions on this issue are illustrated by various examples supplied by a simple program code on MATLAB, which can be easily modified by non-professional users. The readers who may wish to study the problem further can validate numerical data, given in the book, using computer calculations. Thus, they will be able to understand the details of the algorithm and, if necessary, modify computer programs.

References

1. Dubrovkin, J., Belikov, V. *Derivative spectrometry: Theory, Technology, and Application*. Rostov: Rostov University. 1988. [Russian].
2. Talsky .G. *Derivative spectrophotometry: low and high order*. VCH. 1994.
3. Workman Jr., J. J., Mobley, P. R., Kowalski, B. R., Bro, R. (1996). Review of Chemometrics Applied to Spectroscopy: 1985-95, Part 1. Applied Spectroscopy Reviews, 31, 73-124.
4. Mobley, P. R., Kowalski, B. R., Workman Jr., J. J., Bro, R. (1996). Review of Chemometrics Applied to Spectroscopy: 1985-95, Part 2. Applied Spectroscopy Reviews, 31, 347-368.
5. Mark, H., Workman, Jr. *Chemometrics in Spectroscopy*, ELSEVIER. 2007.
6. Brereton, R. G. *Applied Chemometrics for Scientists*. Wiley. 2007.
7. Dubrovkin, J. *Mathematical processing of spectral data in analytical chemistry: A guide to error analysis*. Cambridge Scholars Publishing. 2018.

ABOUT THE STRUCTURE OF THE BOOK

The book is organized into five parts. In the first part, mathematical derivatives of analytical signals are discussed together with the resolution enhancement and information aspects of derivative spectroscopy. The second part is dedicated to analog and numerical differentiation (difference method, Savitzky-Golay filters, Fourier transform, spline, and wavelet processing). The subjects of the two chapters are modulation spectroscopy based on optical monochromators and lasers. In Parts III and IV, derivative qualitative and quantitative analyses, illustrated by numerous examples, are discussed. The final bibliography part briefly describes hundreds of applications of the derivative spectroscopic and non-spectroscopic methods in the industrial and research laboratories.

We sincerely apologize to all those researchers whose outstanding works are not cited because the book does not have enough free space to include a complete bibliography. The project "Derivative Spectroscopy" (https://www.researchgate.net/profile/Joseph_Dubrovkin) provides a bibliographical supplement, which will be updated as new information becomes available.

The author wants to give each chapter status of an article whose reading is independent of other sections. This material presentation allows readers to avoid cramming a previous text before moving on to another topic. MATLAB-based examples, which are focused on the subject matter, illustrate each chapter.

The book closes with appendices, which include supplementary materials necessary to facilitate the readers' ability to understand the theoretical problems, which are discussed in the main text more deeply. For example, a brief introduction to the mathematical method such as Fourier transform, spline approximation, and Tikhonov regularization is given. Technical features of the analog RC devices are discussed. The laser diodes working principles are reviewed. One appendix summarizes, in brief, the main principles and instrumentation of optical spectrometry. However, for clarity, some details of the issue are given in the main text.

Reading requires the knowledge of the secondary school courses on differential calculus, linear algebra, and statistics. To perform the exercises, readers must have programming skills for beginners in MATLAB.

Appendix SW includes some supplementary programs needed for the exercise. Also, the project "Derivative Spectroscopy" (https://www.researchgate.net/profile/Joseph_Dubrovkin) provides open-source MATLAB files.

A significant part of the book is based on the original research carried out by the author.

For simplicity, the captions of figures, tables, exercises, and expressions have the following structure: "part.Chapter-current number."

The author would be very grateful for the criticisms, comments, and proposals about this book, which he hopes to consider in his future work.

ABBREVIATIONS

AAS- Atomic Absorption Spectrometer (Spectrometry)	EPR- Electron Paramagnetic Resonance
AC-Analytical Signal	EXAFS- Extended X-Ray Absorption Fine Structure
AES- Auger Electron Spectra	FAAS-Flame AAS
AFS-Atomic Fluorescence Spectroscopy	FD- Fractional Derivative
AM-Amplitude Modulation	FM-Frequency Modulation
ATF-AAS Atom-Trapping Flame AAS	FT-Fourier Transform
CARS- Coherent Anti-Stokes RS	FTIR-Fourier Transform Infrared Spectroscopy
CCD- Charge-Coupled Device	FWHM-Full Peak Width at Half-Maximum
CFT- Continuous Fourier Transform	GDH-Generalized Discrete Harmonics
CVAAS- Cold Vapour AAS	GFAAS- Graphite Furnace AAS
CWT- Continuous Wavelet Transform	GFT- Generalized Fourier Transform
DBR- Distributed Bragg Reflector	HA-Harmonic Analysis
DCP-Diclorophenol	HGAAS- Hydride-generation AAS
DCVA-Derivative Cyclic Voltabsorptometry	IFT-Inverse FT
DFB-Distributed Feedback Architecture	IM-Intensity Modulation
DFT-Discrete Fourier Transform	ICP-OES- Inductively Coupled Plasma Optical Emission Spectroscopy
DHS-Double Heterostructure	IT- Information Theory
DIR-Derivative IR	LC/MS- Liquid-Chromatography-Mass Spectrometry
DLSVA-Derivative Linear Sweep Voltabsorptometry	IR- Infrared
DPP- Diphenylpropane	LF-Laser Fluorimetry
DSC-Differential Scanning Calorimetry	LIBS-Laser-Induced Breakdown Spectroscopy
DSP-Digital Signal Processing	LMS-Laser Modulation Spectroscopy
DWOD-Dual-Wavelength Optical Differentiation	LTCM- Linear Transform Coordinates Methods
EFM-Electrochemical FM	MDSC- Modulation DSC
EOM-Electro-Optic Phase Modulator	MPI -Multiphoton Ionization

MS- Modulation Spectroscopy	VIS-Visible
MW-Microwaves	WM-Wavelength Modulation
NAS-Net Analyte Signal	WT-Wavelet Transform
NLDM-Natural Logarithm	XAES-X-Ray Excited AES
Derivative Method	XANES-X-ray Absorption Near-Edge Structure
oCPA-Orto-Chlorophenoxyacetic Acid	XS-X-Ray Spectroscopy
OLS-Ordinary Least Squares	XAS-X-Ray Absorption Spectroscopy
OPO-Optical Parametric Oscillator	XDS-X-Ray Diffuse Scattering Spectroscopy
OTM-Orthogonal Transformation Method	XES-X-Ray Emission Spectroscopy
QCL-Quantum-Cascade Lasers	XPS-X-Ray Photoelectron Spectroscopy (Spectrum)
PAS-Photoacoustic Spectroscopy	
PCA-Principal Component Analysis	
pCPA- para-Chlorophenoxyacetic Acids	
PMG- Polynomial Modified Gaussian function	
PT- Pettrash Resolution Criterion	
REMPI-Resonant Enhanced MPI	
RDS-Raman Difference Spectroscopy	
RF-Radio Frequency	
RS-Raman Spectrum	
RW-Radio Waves	
SERDS-Shifted Excitation RDS	
SFS-Synchronous Fluorescence Spectroscopy	
SG-Savitzky-Golay	
SGF-SG Filters	
S/N-Signal-to-Noise Ratio	
SP-Sparrow Resolution Criterion	
SVD-Singular Value Decomposition	
TR-Tikhonov Regularization	
UV-Ultraviolet	

PART I:

MATHEMATICAL DERIVATIVES OF

ANALYTICAL SIGNALS

INTRODUCTION

According to Danzer [1], analytical signal (AS) in analytical chemistry is a response of the measurement system (analytical instrument) to the object under study [1]. Usually, the system's output is a linear or nonlinear mixture of the responses to different analytes, including noise and background.

In terms of signal processing theory, AS "refers to either a continuous or discrete measurement sequence which consists of a pure or undistorted signal corrupted by noise" [2]. In spectroscopy, this measurement sequence is usually a function of the frequency or wavelength. These arguments are, in turn, also time functions. In chromatography, the x-axis (abscissa) of the AS is often time. AS processing is carried out in the time scale of coordinate x (the time domain) or the transformed x-scale, e.g., using the Fourier transform (FT) (the frequency domain). In the last case, the y-coordinates of the AS are the intensity of the Fourier harmonics. Each harmonic is a linear combination of the AS ordinates.

The y-axis of the AS may be the derivatives of the AS relative to the x-argument. Therefore, signal processing in the time domain involves the extraction of useful information from the transformed y-coordinate system. This method, e.g., derivative spectroscopy or chromatography, is one of the Linear Transform Coordinates Methods (LTCM) [3].

Before studying the properties of the derivative methods, let us consider the shapes of the AS components and characteristics of the measurement noise. For simplicity, the AS structural elements, which have a bell-shaped form (symmetrical and asymmetrical), are named peaks.

CHAPTER ONE

SYMMETRICAL PEAK SHAPES IN SPECTROSCOPY AND CHROMATOGRAPHY

In spectroscopy [4] and chromatography [5], a conventional model of AS is a sum of elementary peaks and a baseline. The peaks have symmetrical (Gaussian, Lorentzian, and Voigt) and asymmetrical [6-7] bell-shaped forms. These shapes are due to the impact of physical and instrumental factors. The last effects are essential in chromatography. Some asymmetrical peak shapes and their derivatives are considered in the next chapter.

Spectral lines have "a natural width" due to the expansion of energy levels according to the Heisenberg uncertainty principle [8]. However, this width is negligible. The following effects cause the lines to become broader: the Zeeman Effect, thermal Doppler broadening, collisional, broadening, and velocity broadening [8].

A significant contribution to the spectral contour formation is made by the thermal motion and interactions between the particles of the object under study. The first factor causes Doppler broadening due to changes in the frequency of the radiation emitted or absorbed by the moving particles.

The instrumental distortions include:

- The limited maximum delay time in the interferogram, which is obtained using Fourier-transform infrared spectrometers, and the non-zero width of the instrumental function of monochromators.
- Inter- and/or intra-atomic and molecular interactions in the samples under study (e.g., Stark broadening in dense plasma [9]; spin-spin interactions in NMR spectroscopy [10]; and inter- and intra-molecular associations in IR spectroscopy of liquids [11]).

Doppler broadening forms the Gaussian contour [8] (Fig. 1.1-1):

$$F_G(\lambda) = F_0 \exp\{-4\ln 2[(\lambda - \lambda_0)/w]^2\}, \quad (1.1 - 1)$$

where λ is the abscissa argument with a dimension (e.g., a wavenumber); F_0 is the value of the peak maximum whose position is λ_0 ; and w is the full peak width on the half-maximum (FWHM). The frequently used peak model in chromatography is the Gaussian type.

Interactions between particles form the Lorentzian (or Cauchy) contour [8] (Fig. 1.1-1):

$$F_L(\lambda) = F_0 \{1/[1 + 4[(\lambda - \lambda_0)/w]^2]\}. \quad (1.1 - 2)$$

In physics, the functions $F_G(\lambda)$ and $F_L(\lambda)$ are usually normalized to the unit area:

$$M_G \int_{-\infty}^{\infty} F_G(\lambda) d\lambda = 1.$$

Since $\int_{-\infty}^{\infty} F_G(\lambda) d\lambda = F_0 \sqrt{\pi} w / 2\sqrt{\ln 2}$ [12], $M_G = 2\sqrt{\ln 2 / \pi} / (w F_0)$.

$$M_L \int_{-\infty}^{\infty} F_L(\lambda) d\lambda = 1.$$

Since $\int_{-\infty}^{\infty} F_L(\lambda) d\lambda = F_0 \pi w / 2$ [12], $M_L = (2/\pi) / (w F_0)$.

Each spectrum measured by a spectral instrument is disturbed by this device. From a mathematical point of view, the measured ($F_m(\lambda)$) spectrum is the convolution of the undistorted ("true") spectrum (F_T) with the instrumental function (I) [13]:

$$F_m(\lambda) = \int_{-\infty}^{\infty} I(\lambda + \lambda') F_T(\lambda') d\lambda' + \eta(\lambda), \quad (1.1 - 3)$$

where $\eta(\lambda)$ is the additive noise of the measurements.

Formally, the generalized function (I_g) (which includes instrumental factors) also considers the physical-chemical interactions caused by the distortions of the spectrum under study. According to [14], the undisturbed spectrum equals the measured one corrected by its weighted derivatives:

$$F_T(\lambda) = F_m(\lambda) + \sum_{n=1}^{\infty} (b_n / j^n) d^n F_m(\lambda) / d\lambda^n, \quad (1.1 - 4)$$

where constants b_n are defined by $I_g, j = \sqrt{-1}$.

Shapes of the spectral peaks, measured in practice, often differ from the "pure" functions (Eqs. (1.1-1, 1.1-2)) due to the combined impact of broadening factors and instrumental distortions. Therefore, the peaks are approximated by the Voigt profile, which is the convolution of Gaussian and Lorentzian shapes:

$$F_V(\lambda) = \int_{-\infty}^{\infty} F_G(\lambda') F_L(\lambda - \lambda') d\lambda'. \quad (1.1 - 5)$$

The precise approximation of the Voigt FWHM with an accuracy of 0.02% [15]:

$$w_V = 0.5346w_L + \sqrt{0.2166w_L^2 + w_G^2}. \quad (1.1 - 6)$$

There were some attempts to obtain non-integral analytical expressions of the Voigt function. However, these expressions are cumbersome; for example, the pseudo-Voigt normalized profile [16], and its improved version [17]. Approximation of Voigt function combined two expressions, one of which was an asymptotic [18]. Software products used many rough but simplified combinations of Gaussian and Lorentzian profiles (e.g., [19]).

The Voigt function and its derivatives were represented by series in Hermite polynomials [20].

Fig. 1.1-1 shows the intermediate position of the Voigt peak between the Lorentzian and Gaussian profiles.

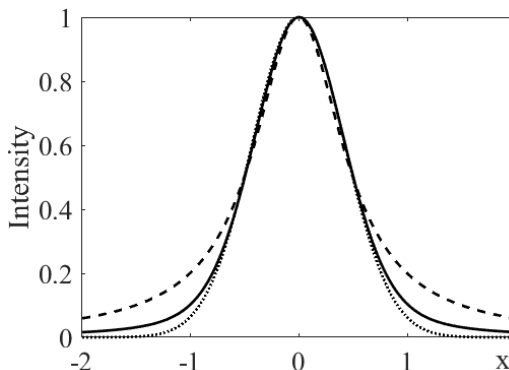


Figure 1.1-1. Lorentz, Gauss, and Voigt peaks (dashed, dotted, and solid curves, respectively). $F_0 = 1$, $x = (\lambda - \lambda_0)/w$, $w = 1$.

Exercise 1.1-1

The readers are invited to study the following:

1. The dependence of the Voigt peak width on the ratio w_L/w_G , using the program VoigtTest.m (Appendix Software SW1).
2. The rough approximation of Voigt peak: $F_L * F_G$. For this purpose, the program VoigtTest.m. must be slightly modified.

For the convenience of mathematical operations, Eqs. (1.1-1) and (1.1-2) are replaced by their Fourier transforms (FT) (Appendix A):

$$\tilde{F}_G(p) = F_0 w_G (\sqrt{\pi} / 2\sqrt{\ln 2}) \exp(-p^2 / 16\ln 2), \quad (1.1 - 7)$$

$$\tilde{F}_L(p) = F_0 w_L(\pi/2) \exp(-|p|/2), \quad (1.1-8)$$

where $p = \omega w$, and ω is the angular (Fourier) frequency.

It is assumed that $\lambda_0 = 0$. If $\lambda_0 \neq 0$, then the FT is modified:

$$F(\lambda - \lambda_0) \rightarrow \tilde{F}(\omega) \exp(-j\omega\lambda_0). \quad (1.1-9)$$

The FT of the Voigt peak is the product of the FT-convolution components normalized to the maximum intensity or area:

$$\tilde{F}_V = \tilde{F}_G * \tilde{F}_L. \quad (1.1-10)$$

CHAPTER TWO

MATHEMATICAL DERIVATIVES OF TYPICAL PEAKS

Analysts usually perform modelling experiments using numerical data to study peculiarities of the qualitative and quantitative analysis based on the derivative methods. For example, the n -order derivative of a composition of the overlapping symmetrical Gaussian, Lorentzian, or Voigt peaks simulated a real analytical signal in spectroscopy. In chromatography, the asymmetrical shapes are usually used. Often the model is corrupted by random noise. These data obtained by the digital differentiation are disturbed by processing errors depending on the differentiation method, sampling interval, and noise. Therefore, only approximate information is extracted from the derivatives. Moreover, the resolution of the derivative peaks essentially depends on the accuracy of the differentiation.

To estimate the properties of the derivative methods accurately, first of all, we intend to carry out theoretical studies using analytical expressions of the mathematical derivatives of the typical peak shapes, both symmetrical and asymmetrical. Often, the roots and the extrema of the derivatives peaks are established analytically. However, generally, this accurate information is readily extracted numerically.

Despite the apparent simplicity, analytical differentiation of mathematical functions, describing model peaks, requires a smart algebraic technique.

Theoretical studies also use analytical expressions of the mathematical derivatives, e.g., for estimating the resolution limit.

Symmetrical peaks

Let us obtain accurate analytical expressions of the mathematical derivatives of the Gaussian (Eq. (1.1-1)) and Lorentzian (Eq. (1.1-2))

peaks. In the first case, we use the physicists' Hermite polynomials [1, 2]:

$$H_n(y) = (-1)^n \exp(y^2) \frac{d^n}{dy^n} \exp(-y^2). \quad (1.2 - 1)$$

$$H_n(y) = n! \sum_{m=0}^{\lfloor \frac{n}{2} \rfloor} \frac{(-1)^m}{m!(n-2m)!} (2y)^{n-2m}. \quad (1.2 - 2)$$

For example,

$$H_0(y) = 1,$$

$$H_1(y) = 2y,$$

$$H_2(y) = 4y^2 - 2,$$

$$H_3(y) = 8y^3 - 12y,$$

$$H_4(y) = 16y^4 - 48y^2 + 12,$$

$$H_5(y) = 32y^5 - 160y^3 + 120y,$$

$$H_6(y) = 64y^6 - 480y^4 + 720y^2 - 120,$$

$$H_7(y) = 128y^7 - 1344y^5 + 3360y^3 - 1680y.$$

Table 1.2-1. Zeros of Hermite polynomials [2]

Order					
1	2	3	4	5	6
0	± 0.7071	0 ± 1.22474	± 0.52464 ± 1.65068	0 ± 0.95857 ± 2.02018	± 0.43607 ± 1.33584 ± 2.35060

From Eqs. (1.2-1) and (1.1-1) we have

$$F_0 \frac{d^n}{dy^n} \exp(-y^2) = \frac{d^n}{dy^n} F_G(y) = (-1)^n H_n(y) F_G(y), \quad (1.2 - 4)$$

where $y = 2\sqrt{\ln 2}(\lambda - \lambda_0)/w$.

The derivative over λ :

$$\frac{d^n}{d\lambda^n} F_G(\lambda) = (2\sqrt{\ln 2}/w)^n \frac{d^n}{dy^n} F_G(y). \quad (1.2 - 5)$$

Instead of cumbersome direct sequential differentiation of the Lorentz shape, we first transform Eq. (1.1-2),

$$F_L(y) = 0.5 F_0 [1/(1+jy) + 1/(1-jy)], \quad (1.2 - 6)$$

where $j = \sqrt{-1}$.

The n^{th} -order derivative of Eq. (1.2-6) is

$$F_L^{(n)}(y) = F_0 (-1)^n (n!/2) [j^n/T_1 + (-j)^n/T_2] = \\ F_0 (-j)^n (n!/2) \{ [(-1)^n T_1 + T_2]/(1+y^2)^{n+1}\}, \quad (1.2 - 7)$$

where $T_1 = (1+jy)^{n+1}$, $T_2 = (1-jy)^{n+1}$.

Using the binomial formula [3], we transform the nominator of Eq. (1.2-7) (omitting F_0):

$$(n! / 2) \sum_{k=0}^{n+1} C_{n+1}^k j^{k+n} y^k [(-1)^{k+n} + 1], \quad (1.2 - 8)$$

where $C_{n+1}^k = (n+1)!/[k!(n+1-k)!]$.

The term

$$(-1)^{k+n} + 1 = \begin{cases} 0, & k+n \text{ is odd}, \\ 2, & k+n \text{ is even}. \end{cases} \quad (1.2 - 9)$$

Taking Eq. (1.2-9) into account, we have from Eq. (1.2-8):

$$n \quad \text{Eqs. (1.2-10)}$$

$$1 \quad C_2^1 j^2 y = -2y$$

$$3 \quad 3! (C_4^1 j^4 y + C_4^3 j^6 y^3) = 24y - 24y^3$$

$$5 \quad 5! (C_6^1 j^6 y + C_6^3 j^8 y^3 + C_6^5 j^{10} y^5) = 5! (-6y + 20y^3 - 6y^5)$$

$$7! (C_8^1 j^8 y + C_8^3 j^{10} y^3 + C_8^5 j^{12} y^5 + C_8^7 j^{14} y^7) =$$

$$7! (8y - 56y^3 + 56y^5 - 8y^7) = 7! y(y^2 - 1)(-y^4 + 6y^2 - 1)$$

$$2 \quad 2(C_3^0 j^2 + C_3^2 y^2) = -2 + 6y^2$$

$$4 \quad 4! (C_5^0 j^4 + C_5^2 j^6 y^2 + C_5^4 j^8 y^4) = 24(1 - 10y^2 + 5y^4)$$

$$6 \quad 6! (C_7^0 j^6 + C_7^2 j^8 y^2 + C_7^4 j^{10} y^4 + C_7^6 j^{12} y^6) = \\ 6! (-1 + 21y^2 - 35y^4 + 7y^6)$$

The roots of Eqs. (1.2-10) are readily obtained analytically except $n = 6$.

The derivatives of Lorentzian peaks over λ :

$$\frac{d^n}{d\lambda^n} F_L(\lambda) = (2/w)^n \frac{d^n}{dy^n} F_L(y). \quad (1.2 - 11)$$

Figure 1.2-1 represents the plots of the Gaussian and Lorentzian peaks and their derivatives up to the sixth order. Zero points of the derivatives $\Delta\lambda_r/w = (\lambda - \lambda_r)/w$ (Table 1.2-2) are the roots of Eqs. (1.2-3) and (1.2-10). They were obtained analytically and numerically.

The intensity of the n^{th} -order derivative (Eqs. (1.2-5) and (1.2-11))

$$F^{(n)} \sim w^{-n}. \quad (1.2 - 12)$$

So, the differentiation redistributes intensities in favor of narrow peaks.

It follows from Eqs. (1.2-3), (1.2-5), (1.2-10), and (1.2-11) that in the central point $y = 0$ of the even-order derivatives,

$$F_G^{(n)}(0) = (-4\ln 2)^{n/2} n! / (n/2)!$$

$$F_L^{(n)}(0) = (-4)^{n/2} n! \quad (1.2 - 13)$$

for the Gaussian and Lorentzian peaks, respectively.

The extrema $\Delta\lambda_e/w = (\lambda - \lambda_e)/w$ and $F_e^{(n)}w^n/F_0$ (Table 1.2-2) were evaluated numerically.

In further calculations, we use the following ratios estimated for the 3rd-, 5th-, and 7th-order derivatives in the extrema y_{e1} of the 1st-order derivatives of the Gaussian and Lorentzian peaks:

$$\begin{aligned} F_G^{(n)}(y_{e1})/F_G^{(1)}(y_{e1}) &= 11.09, 184.56, 3413.4; \\ F_L^{(n)}(y_{e1})/F_L^{(1)}(y_{e1}) &= 18.00, 0, 136.08 \times 10^3. \end{aligned} \quad (1.2 - 14)$$

Exercise 1.2-1

Readers are invited to do the following:

- Obtain the final formulas for the derivatives of the Gaussians and Lorentzians.
- Answer the following questions using Figure 1.2-1 and Table 1.2-2:
 - a) What are the orders of the derivative curves which resemble the original peak?
 - b) What information can you extract from zero and the extrema points?
 - c) What can you tell about the properties of the central components of the even-order derivatives and additional side structures called satellites?
 - d) Estimate the narrowing of the central peaks of the even-order derivatives.
 - e) Estimate the form parameter [4]: the intensity ratios of the central peaks to the satellites of the even-order derivatives.

To estimate the signal-to-noise ratio of derivatives, we need the amplitude sweep, that is, the maximum distance between the extrema points ($F_e^{(n)}$):

$$\Delta D^{(n)} = |D_{Max}^{(n)}| + |D_{Min}^{(n)}|, \quad (1.2 - 15)$$

where $D_e^{(n)} = F_e^{(n)}w^n/F_0$.

From Table 1.2-2, we have

$$\begin{aligned} \Delta D_G^{(1)} &= 2 \times 1.4283 = 2.8566; \\ \Delta D_G^{(2)} &= 5.5452 + 2.4746 = 8.0198; \\ \Delta D_G^{(4)} &= 92.2470 + 57.0353 = 149.2823. \end{aligned} \quad (1.2 - 16)$$

$$\begin{aligned} \Delta D_L^{(1)} &= 2 \times 1.2990 \approx 2.6; \\ \Delta D_L^{(2)} &= 8 + 2 = 10; \end{aligned}$$

$$\Delta D_L^{(4)} = 384 + 162 = 546.$$

Let us use the Fourier transform (Appendix A) to estimate the integral intensity of the derivatives:

$$\tilde{F}^{(n)}(\omega) = \int_{-\infty}^{\infty} F^{(n)}(\lambda) \exp(-j\omega\lambda) d\lambda, \quad (1.2 - 17)$$

where ω is the angular (Fourier) frequency, $j = \sqrt{-1}$.

Since $\tilde{F}^{(n)}(\omega) = (j\omega)^n \tilde{F}(\omega)$, $\tilde{F}^{(n)}(0) = 0$ if $n > 0$.

So, we have from Eq. (1.2-17):

$$\tilde{F}^{(n)}(0) = \int_{-\infty}^{\infty} F^{(n)}(\lambda) d\lambda = 0. \quad (1.2 - 18)$$

That is, the integral intensity of the derivative curves is zero. Therefore, the areas under their positive and negative peaks are equal.

The value of the area under the unipolar derivative peaks was a measure of the analyte amount in the quantitative analysis (Chapter 4.1).

Asymmetrical peaks

There are a lot of mathematical models of asymmetrical peaks usually used in chromatography [5]. As examples, consider the polynomial modified Gaussian (PMG) and Lorentzian (Dobosz) functions.

The PMG function and its derivatives:

$$F_{PMG} = \exp(-y^2/B_y^2). \quad (1.2 - 19)$$

$$F_{PMG}^{(1)} = C_1 y F_{PMG}, \quad (1.2 - 20)$$

$$F_{PMG}^{(2)} = C_1 [(1 - 3\tau y) F_{PMG}/B_y + y F_{PMG}^{(1)}] = C_2 F_{PMG} \Phi, \quad (1.2 - 21)$$

$$F_{PMG}^{(3)} = C_2 [(F_{PMG}^{(1)} - 6\tau F_{PMG}/B_y) \Phi - F_{PMG} (4y + 6\tau^2 y B_y)], \quad (1.2 - 22)$$

where $y = 2\sqrt{\ln 2}(\lambda - \lambda_0)/w$; $C_1 = -2/B_y^3$; $C_2 = -2/B_y^6$;

B_y is $= 1 + \tau y$; τ the asymmetry parameter; $\Phi = B_y^3 - 3\tau y B_y^2 - 2y^2$.

Exercise 1.2-2

Readers are invited to validate that Eqs. (1.2-19)-(1.2-22) describe the Gaussian peak and its derivatives if $\tau = 0$.

Analytical expressions of the derivatives, with an order higher than 3, are more cumbersome. Appendix B1 describes sequential high-order differentiation of the PMG peak.

Figure 1.2-2 shows that the right asymmetrical tail of the high-order derivatives of slightly skewed PMG peak ($\tau = 0.05$) is strongly distorted

compared to the symmetrical wing of corresponding Gaussian shape derivatives. Table 1.2-3 summarizes the quantitative parameters of the PMG shape derivatives. Numerical errors caused small discrepancies between zeros and the extrema positions in the derivatives of $n + 1$ - and n -order, respectively.

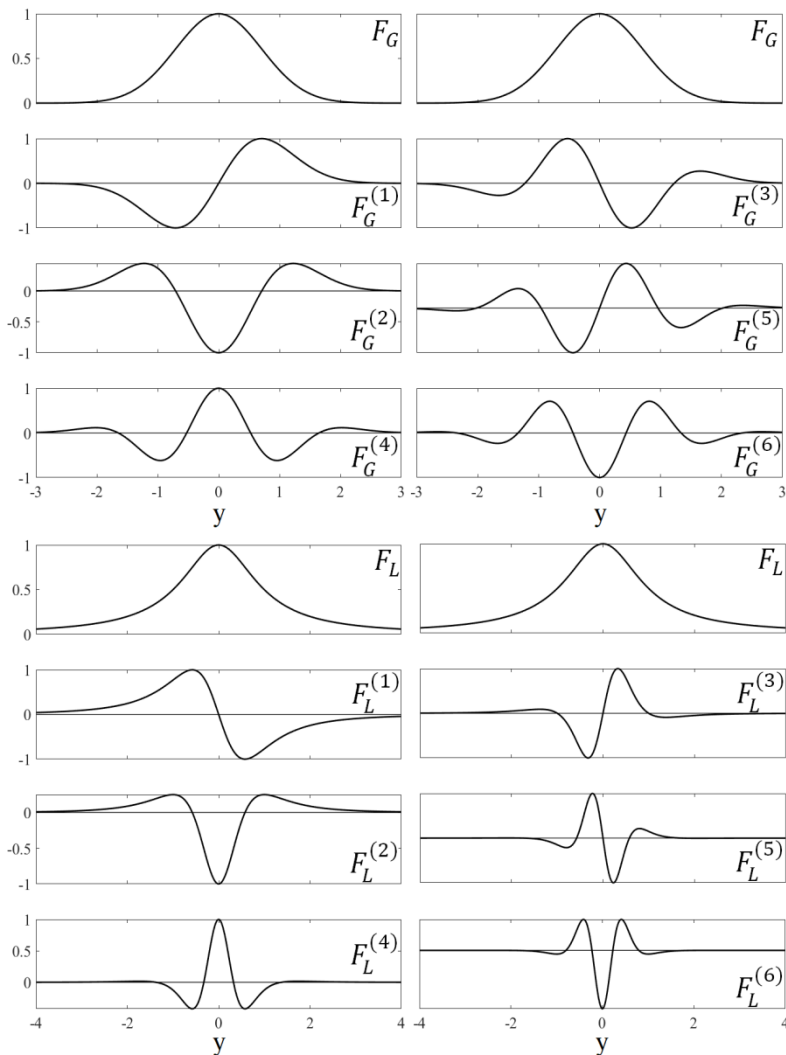


Figure 1.2-1. Plots of the normalized derivatives.

Table 1.2-2. Parameters of the derivatives

<i>n</i>	Peak							
	Gaussian				Lorentzian			
	$\frac{\Delta\lambda_r}{w}$	$\frac{\Delta\lambda_e}{w}$	$\frac{F_e^{(n)} w^n}{F_0}$	$ \varphi^{(n)} ^*$	$\frac{\Delta\lambda_r}{w}$	$\frac{\Delta\lambda_e}{w}$	$\frac{F_e^{(n)} w^n}{F_0}$	$ \varphi^{(n)} ^*$
1	0	± 0.425	± 1.428	-	0	± 0.289	± 1.299	
2	± 0.425	0 ± 0.736	-5.545 2.475	2.241	± 0.289	0 ± 0.500	-8 2	4
3	0 ± 0.736	± 0.315 ± 0.992	± 18.0 ± 4.90	-	0 ± 0.5009	± 0.163 ± 0.689	± 37.349 ± 3.368	
4	± 0.315 ± 0.991	0 ± 0.576 ± 1.213	92.3 -57.0 10.7	1.617 8.603	± 0.163 ± 0.688	0 ± 0.289 ± 0.867	384 -162 6	2.37 64
5	0 ± 0.576 ± 1.213	± 0.262 ± 0.802 ± 1.412	± 418.7 ± 182.6 ± 25.5	-	0 ± 0.289 ± 0.867	± 0.114 ± 0.399 ± 1.038	± 3214.7 ± 685.7 ± 11.4	-
6	± 0.262 ± 0.802 ± 1.412	0 ± 0.490 ± 1.005 ± 1.593	-2557.6 1812.4 -599.1 65.2	1.411 4.269 39.23	± 0.114 ± 0.399 ± 1.038	0 ± 0.207 ± 0.500 ± 1.207	-46080 24459 -2880 21	1.88 16.0 2194

* The form parameter $\varphi^{(n)} = \left| F_e^{(n)} \right|_{max} / F_e^{(n)}$.

It follows from Table 1.2-3 that:

- The shift of the central minimum of the 2nd-order derivatives is approximately $-\tau$. Let us show that this result follows from Eq. (1.2-22). Since, near the minimum (y_e) y and τy are close to zero, $B_y \cong 1$, $F_{PMG}^{(1)} \cong -2y$, $F_{PMG} \cong 1$; for $\tau \ll 1$, $\tau^2 y \cong 0$, $\tau y^2 \cong 0$. By zeroing Eq. (1.2-22), we have

$$F_{PMG}^{(3)} \cong 4[(y + 3\tau)(1 - 3\tau y) + 2y] \cong 4y + 12\tau + 8y = 0. \quad (1.2 - 23)$$

So, $y_e \approx -\tau$.

2. The shift of the central peak of the 4th-order derivatives is roughly two times larger than that of the 2nd-order derivative.
3. The left- and the right-side form parameters (the absolute ratios of the satellite intensity to the intensity of the central peak in the 2nd-order derivatives) are unequal.

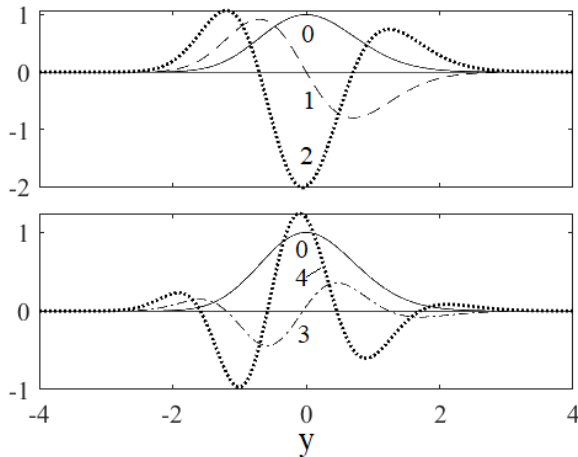


Figure 1.2-2. PMG peak and its derivatives. Numbers near curves designate the differentiation order. $\tau = 0.05$. $F_{PMG}^{(3)}$ and $F_{PMG}^{(4)}$ are multiplied by 0.1.

Asymmetrical Lorentzian (Dobosz) function:

$$F_D = \exp(-\tau(1 - \tan^{-1}y)) F_L = C \exp(K_y) * K_y^{(1)}, \quad (1.2 - 24)$$

where $\tau \neq 0$; $F_L = 1/(1 + y^2)$; $C = \exp(-\tau)/\tau$; $K_y = \tau \tan^{-1}y$;

$$K_y^{(1)} = \tau F_L.$$

$$F_D^{(1)} = C \exp(K_y) \left[(K_y^{(1)})^2 + K_y^{(2)} \right] = C \exp(K_y) T_y, \quad (1.2 - 25)$$

$$K_y^{(2)} = -2\tau y F_L^2, \quad T_y = \tau[(\tau - 2y)] F_L^2,$$

$$F_D^{(2)} = F_D T_y + C \exp(K_y) T_y^{(1)}, \quad (1.2 - 26)$$

$$T_y^{(1)} = \tau(6y^2 - 4\tau y - 2) F_L^3.$$

Analytical expressions of the n^{th} -order derivatives, for $n > 2$, are more cumbersome. Appendix B1 describes sequential high-order

differentiation of the PMG. Tables 1.2-3 and 1.2-4 summarize the quantitative parameters of the Dobosz shape derivatives.

It follows from Table 1.2-4 that the Dobosz peak maximum is shifted by $\tau/2$. This result is obtained by zeroing the term T_y (Eq. (1.2-25)). The shift of the PMG peak is zero. The central peaks of the Dobosz shape 2nd- and the 4th-order derivatives are shifted approximately by $\tau/3$ and $\tau/4$, respectively (Table 1.2-4). Therefore, we suppose that impact of the asymmetry on the uncertainty in determining maximum of the polynomial modified Lorentzian asymmetrical peaks is significantly smaller than those of the asymmetrical Gaussians.

The form parameters of the 2nd-order derivatives of the PMG and Dobosz peaks (Table 1.2-5) are highly-sensitive to the asymmetry parameter τ . If τ increases, then the right-side satellite significantly decreases compared to the one on the left-side.

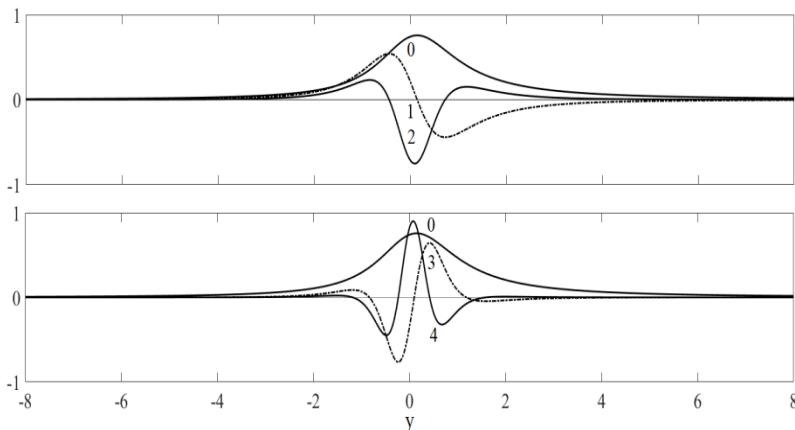


Figure 1.2-3. Dobosz peak and its derivatives. Numbers near curves designate the differentiation order. $\tau = 0.3$. $F_{PMG}^{(2)}$, $F_{PMG}^{(3)}$ and $F_{PMG}^{(4)}$ are multiplied by 0.5, 0.2 and 0.05, respectively.

Exercise 1.2-3

Readers are invited to study the dependencies of the positions and amplitudes of the extrema values of the PMG and Dobosz peak derivatives on the asymmetry parameter using Tables 1.2-3 and 1.2-4.

Table 1.2-3. Parameters of the PMG derivatives

<i>n</i>		<i>τ</i>				
		0	0.05	0.10	0.15	0.20
0	<i>y_e</i>	0	0	0	0	0
	<i>F_e⁽⁰⁾</i>	1	1	1	1	1
1	<i>y_r</i>	0	0	0	0	0
	<i>y_e</i>	-0.7070 0.7070	-0.7060 0.7060	-0.7020 0.7020	-0.6960 0.6950	-0.6890 0.6850
	<i>F_e⁽¹⁾</i>	0.8578 -0.8578	0.9206 -0.7992	0.9877 -0.7449	1.0593 -0.6947	1.1352 -0.6483
2	<i>y_r</i>	-0.7071 0.7071	-0.7058 0.7058	-0.7021 0.7016	-0.6963 0.6947	-0.6886 0.6850
	<i>y_e</i>	-1.2250 0 1.2250	-1.1970 -0.0500 1.2460	-1.16050 -0.0980 1.2610	-1.1290 -0.1430 1.2670	-1.0920 -0.1830 1.2650
	<i>F_e⁽²⁾</i>	0.8925 -2.000 0.8925	1.0741 -2.0150 0.7444	1.2948 -2.0601 0.6247	1.5604 -2.1355 0.5287	1.8774 -2.2417 0.4522
3	<i>y_r</i>	-1.2247 0 1.2247	-1.1969 -0.0497 1.2465	-1.1645 -0.0977 1.2608	-1.1290 -0.1426 1.2670	-1.0917 -0.1834 1.2649
	<i>y_e</i>	-1.6510 - 0.5250 0.5200 1.6510	-1.5860 -0.5810 0.4590 1.7070	-1.5200 -0.6300 0.3900 1.7500	-1.4450 -0.6600 0.3150 1.7820	-1.3750 -0.6840 0.2430 1.7960
	<i>F_e⁽³⁾</i>	3.9036 -1.0604 3.9036 -1.0604	1.4811 -4.4086 3.5780 -0.7670	2.0772 -5.1318 3.4025 -0.5643	2.9113 -6.1250 3.3562 -0.4250	4.0609 -7.505 3.4256 -0.3293
4	<i>y_r</i>	-1.6507 -0.5246 0.5246 1.6507	-1.5858 -0.5809 0.4593 1.7071	-1.5162 -0.6263 0.3882 1.7515	-1.4450 -0.6603 0.3149 1.7816	-1.3747 -0.6836 0.2429 1.7962
	<i>y_e</i>	-2.0200 -0.9600 0.9600 2.0200	-1.9130 -1.0030 -0.0990 0.8950 2.1180	-1.8020 -1.0270 -0.1910 0.8160 2.2010	-1.6940 -1.0350 -0.2720 0.7300 2.2620	-1.5910 -1.0300 -0.3400 0.6310 2.2990
	<i>F_e⁽⁴⁾</i>	1.3949 - 7.4195 12.0000 - 7.4195 1.3949	2.3284 -9.6904 12.4240 -6.0209 0.8518	3.9120 -13.2583 13.7447 -5.2177 0.5375	6.5513 -18.7555 16.1121 -4.8363 0.3548	10.86068 -27.1010 19.7894 -4.7749 0.2470

y_r , y_e and $F_e^{(n)}$ are the roots, extrema and their values, respectively.